Forced Convection Heat Transfer for Swaged Mixed Metal Heatsinks

Ahmed Zaghlol, Ken Hermann and James Butler
R-Theta Inc.
Mississauga, Ontario, Canada
Phone: (905) 795-0077
Fax: (905) 795-2508
azaghlol@r-theta.com

Peter Teertstra and Richard Culham
Microelectronics Heat transfer Laboratory
University of Waterloo
Waterloo, Ontario, Canada

ABSTRACT

This paper is an experimental investigation comparing the thermal performance of four heatsink combinations based on the forced convection heat transfer mode. The four designs consist of an all Aluminum, all Copper, Copper baseplate/Aluminum fin and Aluminum baseplate/Copper fin heatsink. Each heatsink was placed within a vertical wind tunnel of Plexiglas walls such that the fins were positioned vertically and parallel to the airflow inside the tunnel. A block heater providing 585 watts and covering 5% of the baseplate was attached to each heatsink. Experiments were performed for a Reynolds number ranging from 720 to 3200. This Reynolds number was based on the fin spacing. The average rise in temperature of ten measured locations was used to calculate the thermal resistance. The all Copper heatsink provided the lowest thermal resistance while the all Aluminum heatsink returned the highest value. The Copper-Base/Aluminum-Fin and Aluminum-Base/Copper-Fin heatsinks showed very similar thermal resistance results for identical approach velocities. The pressure drop through the Copper fin heatsink was found to be higher than through the Aluminum fin heatsink. For small heat source coverage, the experiments show that there is an increase in the performance of the Copper-Base/Aluminum-Fin heatsink due to the higher conductivity of the Copper base. The experiments show that this performance can be matched by increasing the thermal conductivity of the fin material instead, as in the case of the Aluminum-Base/Copper-Fin heatsink.

Keywords:

Forced Convection, Heatsinks, bonded fins, swaging, mixed metals, Copper

INTRODUCTION

It is well known that the useful life and reliability of semiconductors improves with lower operating temperatures. The temperature of a semiconductor junction is the main criterion for its reliability and performance. The semiconductor manufacturer specifies the maximum allowable value for this junction temperature. During energy conversion in a semiconductor, part of the electrical energy is lost via the temperature rise of the semiconductor due to internal resistance. This energy, which is eventually transferred to surroundings of lower temperature, is otherwise known as heat (or heat loss). To maintain the junction temperature at an allowable level it is therefore necessary to remove this heat. Ultimately, this energy ends up being dissipated by a heatsink to the cooler ambient air, which serves as an infinite sink or reservoir for heat dissipation. The temperature rise of the junction above ambient is dependent on the thermal resistance of the path that the heat is required to take in order to reach its destination - the ambient air. Reducing the thermal resistance of the heatsink contributes to the reduction of the thermal resistance of the path.

High temperature and heat dissipation are the factors currently limiting electronic system capabilities. There are two primary applications that require heatsinks: the microprocessor at the PC board level and Power Electronics. With the trend of decreasing package size and increasing heat dissipation, the heat flux therefore also increases. In order to reduce the heatsink thermal resistance, designers use materials with higher thermal conductivity than Aluminum, such as Copper. The use of such metals as in Copper fin/ Aluminum baseplate, Aluminum fin/Copper baseplate and all Copper sinks, help to improve heat spreading.

For low power dissipation and low heat flux applications, extruded heatsinks are the most commonly used sinks due to its cost effectiveness. However, the extrusion process has limitations. When producing high aspect ratio fins, the extrusion die breaks more readily as the fin thickness and fin spacing decreases. For high volume applications, the die-casting manufacturing technique is an alternative due to its low averaged cost. It should be mentioned that high porosity and low purity alloys result in lower thermal conductivity products.

In heatsinks with bonded fins, the base is extruded with slots to allow the insertion of plates or extruded fins. Attaching the fins to the baseplate can be done using thermal epoxy, brazing or “swaging.” Thermal epoxy is the common method used to bond high aspect ratio heatsinks. However, epoxy possesses a very low thermal conductivity as compared to Aluminum so that the thickness should be minimized in order to minimize its thermal impedance. Brazing is a subgroup of welding that takes place at temperatures above the liquid state of a filler

material (450^{o}C) and below the solid state of the base materials. Capillary action plays a major role in filler flow through the joints.

The heatsinks tested in these experiments were bonded using a metal displacement process referred to as "Swaging" . The Swaging process, depicted in *Figure 1*, can be described as a cold forming process, which is used in the fabrication of high fin density heatsinks. Currently, this process involves the placement of fins with a tapered base into a slotted base plate and then the application of a rolling pressure on the opposite sides of each fin. This results in vertical and lateral pressure of the base unit material , which tends to push the fin toward the bottom of the groove in the base. This secure connection provides very good thermal contact between the fins and base and also prevents air and moisture from entering the grooves, thereby preventing corrosion and allowing the heatsink to be anodized.

EXPERIMENTAL APPARATUS AND PROCEDURE

Heatsink Description:

Four heatsink designs were tested. These were the Aluminum base/Aluminum fin (Al B-Al F), Copper base/Aluminum fin (Cu B-Al F), Aluminum base/Copper fin (Al B-Cu F) and Copper base/Copper fin (Cu B-Cu F) sinks as shown in *Figure 2*.

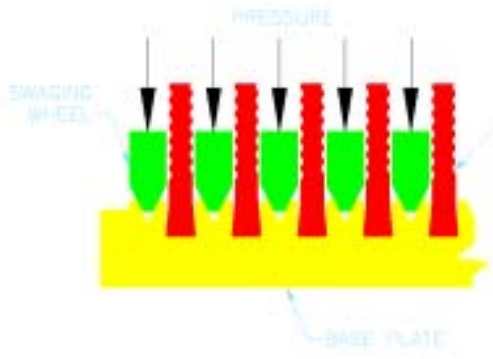

Figure 1: Swaging process of tapered fins into the grooves of a baseplate with the application of rolling pressure on opposite sides of each fin.

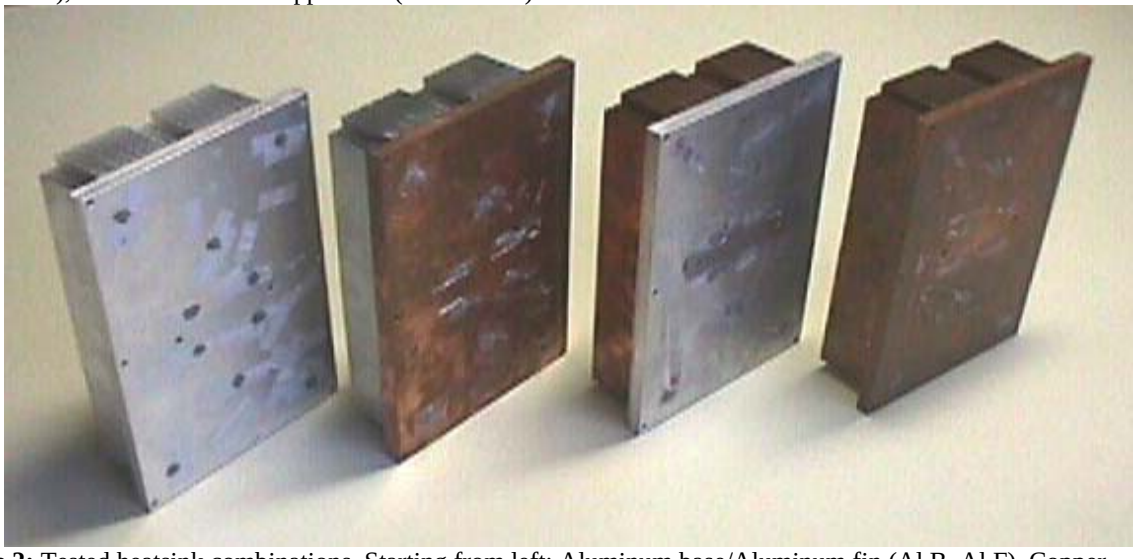

Figure 2: Tested heatsink combinations. Starting from left: Aluminum base/Aluminum fin (Al B–Al F), Copper Base/Aluminum Fin (Cu B–Al F), Aluminum base/Copper Fin (Al B–Cu F) and Copper Base/ Copper Fin (Cu B–Al F).

Generally, the heatsink base plate area, fin height and fin-center-to center distance were the same for all heatsinks as can be seen from *Figure 3 & Table 1*. The Aluminum serrated fins were extruded with an overall average thickness of 1.2 mm and an average base thickness of 1.33 mm. The thicker fin base helps to secure the connection between the fins and the baseplate and results in good thermal contact through the swaging process. The extrusion process used to produce the Aluminum serrated fins is flexible enough to allow for different fin body and fin base geometries as shown in *Figure 4*. For the swaging process involving the flat Copper fins, the (constant)Copper fin thickness was selected to be equal to the Aluminum fin base thickness of 1.33 mm. Copper fins were sheared from 1.33 mm thick rolled flat sheets. The rolling process used to produce Copper plates only allowed for fixed flat sheets (*see Figure 4)*.

Heatsink Assembly

The heatsinks were heated using a 585W pencil heater inserted into an Aluminum block. The heater block dimensions were 19mm 101mm and covered 5% of the heatsink baseplate area. It was assumed that the spreading resistance between the pencil heater and the heatsink base plate was negligible and that the heater surface provided a uniform heat flux of 30.5 W/cm^{2}. Thermal grease, with a thermal conductivity of 0.8 W/mK, was used between the block heater and the heatsink baseplate. A typical line voltage of 132.8 VAC at a current of 4.4A was used to power the heater.

Table 1: Heatsinks geometries and dimensions

Heatsink Model	Al B- Al F	Cu B- Al F	Al B- Cu F	Cu B - Cu F
Baseplate Material	Aluminum	Copper	Aluminum	Copper
Fin Material	Aluminum	Aluminum	Copper	Copper
Fin Profile	Serrated	Serrated	Flat	Flat
Total Heat Transfer Area, A (mm^2)	1137676	11376756	1138237	1138237
X-Sectional Area of Fins, A_f (mm^2)	2587.2	2587.2	2867.5	2867.5
Base Length, L (mm)	253.6	253.6	253.6	253.6
Base Width, W (mm)	153.7	153.7	153.7	153.7
Base Thickness, t_b (mm)	12.7	12.7	12.7	12.7
Fin Height, H (mm)	49	49	49	49
Fin Thickness, t_f(mm)	1.2	1.2	1.33	1.33
Fin to Fin, C-C (mm)	3.43	3.43	3.43	3.43
Fin Spacing, S (mm)	2.23	2.23	2.1	2.1
Fin Height to Fin Spacing Ratio	22:1	22:1	23:1	23:1
Heatsink Weight, kg	3.19	6.53	8.09	11.4
Weight Ratio = (Heatsink Weight)/(Aluminum Heatsink Weight)	1	2.05	2.61	3.57

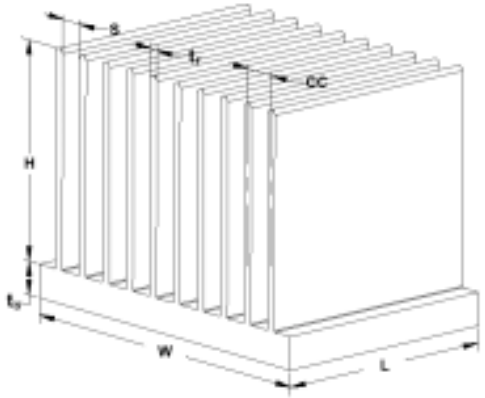

Figure 3: Heatsink geometry and dimensions

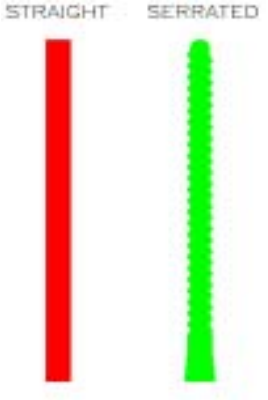

Figure 4: Schematic of serrated and flat fins

In order to facilitate the single heatsink testing without constant substantial disassembly of the test apparatus, a section of the wind tunnel door was modified to allow for a heatsink to be mounted such that the baseplate was flush to the interior wall of the tunnel with the fins extended into the air stream. Large Plexiglas baffles and flow diverters were constructed and positioned in the wind tunnel to ensure a smooth transition of the air into the duct upstream of the heatsink as shown in *Figure 5*. In order to minimize flow bypass effects, the Plexiglas baffles were placed at a distance of approximately 1 fin spacing width, *S* away from the tips of the fins. The entire back of the heatsink was insulated using a 5 cm thick layer of fiberglass insulation to prevent heat losses to the ambient air outside the wind tunnel. In this experimental case of forced convection, the radiation heat transfer component was neglected (less than 1% of total heat dissipated, see Teertstra et al).

Wind Tunnel

Testing of the heatsinks was performed in a vertical, open circuit wind tunnel at the Microelectronics Heat Transfer Laboratory at the University of Waterloo. The wind tunnel, manufactured by Engineering Laboratory Design, had a 24 inch tall by 18 inch x 18 inch cross sectional area test section. A 2 HP, 3-phase motor controlled by a Toshiba VF-SX compact digital inverter powered the blower at the discharge side of the tunnel.

Data Acquisition Instrumentation

Temperature

Heatsink and ambient air temperatures were measured using 36-gauge, T-type Copper-Constantan thermocouples. Ten thermocouples were attached at various locations on the heatsink baseplate as shown in *Figure 6* using Devcon Aluminum-filled epoxy.

Ambient air temperature was measured using two thermocouples at a location upstream from the heatsink. All temperature and voltage measurements were obtained using a Keithley 2700 data acquisition system with a 7700 – 20 channel analog input module. The data logger was controlled using a PC computer connected via a GPIB interface card. The Keithley X-Linx software was used to control the data

logger and to record the measurements. Due to the small diameter of the thermocouple wires and the relatively large values of heat dissipation, conductive and convective losses through the leads were assumed to be negligible.

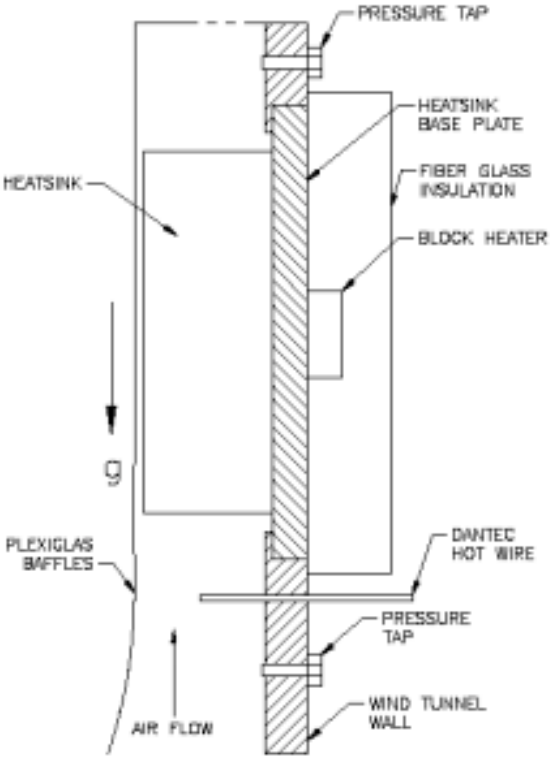

Figure 5: Test section of the heatsink assembly.

Power

The heater was powered by a Xantrex 150 V – 7 A DC power supply. Power dissipated by the heater was calculated based on voltage and current measurements where the current was deduced from a voltage measurement across a calibrated, 10 A shunt resistor.

Velocity

Air velocity was measured in the duct 200mm upstream from the heatsink using a Dantec Flowmaster hot-wire anemometer with a stated accuracy of +/- 0.2 m/s.

Pressure Drop

Pressure drop across the heatsink was measured using two static pressure taps connected to a Dwyer 607 Series Differential Pressure Transmitter, with a range of 0 – 250 Pa and an accuracy of +/- 0.625 Pa.

Measurement Procedure

Once all thermocouples were attached to the heatsink baseplate, the heatsink / test section assembly was placed in the wind tunnel and all instrumentation and power connections were made. Following a brief test to ensure correct operation of all components in the system, testing was performed according to the following procedure:

- The wind tunnel blower was turned on and the frequency of the controller was adjusted such that the first target velocity was reached, as measured by the hot wire anemometer.
- The power supply for the heater was turned on and set to 133 V, a constant value for all subsequent tests.
- After an initial warm-up period and adjustment of the velocity to account for variations in the air density due to heating, the data acquisition system was started.
- Measurements of each of the values were recorded every ten seconds until the following convergence criteria were satisfied:
  1. Minimum time of 30 minutes has elapsed
  2. Less than 0.2 C variation in temperature between 12 subsequent readings (2 minutes)

Once steady state had been achieved, the data was saved, the data acquisition system was reset, the wind tunnel blower was set to the next velocity, and the test was repeated.

DATA REDUCTION

The thermal resistance, R_θ, was calculated as

$$R_\theta = \frac{\overline{T}_S - T_{amb}}{Q} \qquad \textbf{(1)}$$

where

$\overline{T_S}$ *:* average temperature of the heatsink baseplate based on measurement of ten thermocouples [K], shown in *Figure 6*,

$$\overline{T_S} = \left(\sum T_a + \sum T_b + \sum T_c\right)/N \qquad \textbf{(2)}$$

N: number of thermocouples used to measure the baseplate temperature.
$T_{amb:}$ ambient air temperature[K],
Q: total heat transfer rate [W],

The reduction in heatsink thermal resistance as compared to the thermal resistance of the all Aluminum heatsink was measured as follows:

$$\%R_\theta = \frac{R_\theta\big|_{Al\ B-Al\ F} - R_\theta}{R_\theta\big|_{Al\ B-Al\ F}} \times 100 \qquad \textbf{(3)}$$

$R_\theta\big|_{Al\ B-Al\ F}$: thermal resistance of all Aluminum heatsink (Al B-Al F),

Source thermal resistance was expressed as follows:

$$R_{\theta\ Source} = \frac{\overline{T}_a - T_{amb}}{Q} \qquad \textbf{(4)}$$

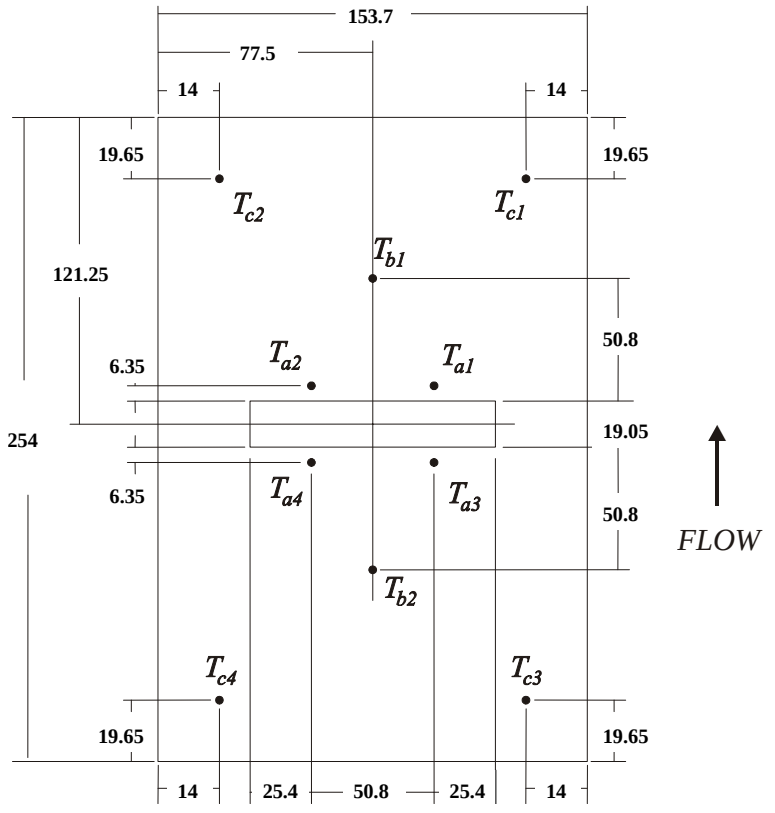

Figure 6: Locations of the thermocouple wires used for temperature measurement on the baseplate.

where

$\overline{T_a}$: average temperature of the four thermocouples located around the heat source [K], *see Figure 6*:

$$\overline{T_S} = \left(\sum T_a\right)/4 \qquad \textbf{(5)}$$

The reduction in source thermal resistance as compared to the all Aluminum source thermal resistance was expressed as follows:

$$\%R_{\theta\ Source} = \frac{R_{\theta\ Source}\Big|_{Al\ B-Al\ F} - R_{\theta\ Source}}{R_{\theta\ Source}\Big|_{Al\ B-Al\ F}} \times 100 \qquad \textbf{(6)}$$

$R_{\theta\ Source}\Big|_{Al\ B-Al\ F}$: source thermal resistance for all Aluminum heatsink (Al B-Al F),

The volumetric airflow rate was calculated as:

$$\overset{o}{V} = V_{\infty} \times A \qquad [m^3/s] \qquad \textbf{(7)}$$

V_{∞}: approach air velocity in the wind tunnel, [m/s]

A: cross sectional area of wind tunnel, [m^2], $A = H \times W$
H: height of wind tunnel duct, [m]
W: width of the wind tunnel duct, [m]

The Reynolds number of the fin channels' airflow, Re_S, was defined as

$$\mathrm{Re}_S = \frac{V_S \cdot 2S}{\nu} \qquad \textbf{(8)}$$

ν: kinematic viscosity of air, [m^2/s]

V_S: air velocity in fin channel,[m/s], $V_S = \overset{o}{V} \Big/ (A - A_f)$
A_f: heatsink cross sectional area, see Table 1, [m^2]
S: width of fin channel i.e. fin spacing, see Table 1, [m]

Nusselt Number Correlation(Teertstra et al 1999):
The experimental average Nusselt number for the heatsink was determined by non-dimensionalizing the total heat transfer rate per channel of the heatsink. The heat transfer per channel was calculated from the total power dissipation Q, divided by the number of channels *(N_f)*, including the two half channels formed between the outer fins and the shroud.

$$Nu_S = \frac{\left(\frac{Q}{N_f}\right) \cdot S}{k(2 \cdot L \cdot H)(\overline{T_S} - T_{amb})} \qquad \textbf{(9)}$$

N_f: number of fins
L: fin length, [m], see Figure 3

Teertstra et al developed an analytical model to predict the average heat transfer rate for forced convection cooled plate fin heatsink based on a combination of the two limiting cases, fully developed and developing flow in a parallel plate channel. Fin effects were included in the model to account for temperature variations between the fins and the baseplate. Combining the fin efficiency model with the solution for the parallel plate channel, the Nusselt number was be expressed as

$$Nu_S = \frac{\tanh\sqrt{2\cdot Nu_i \frac{k_f}{k}\frac{H}{S}\frac{H}{t}\left(\frac{t}{L}+1\right)}}{\sqrt{2\cdot Nu_i \frac{k_f}{k}\frac{H}{S}\frac{H}{t}\left(\frac{t}{L}+1\right)}}\cdot Nu_i \qquad \textbf{(10)}$$

where:
k: thermal conductivity of fin material, [W/mK]
k_f: thermal conductivity of fluid, [W/mK]

$$Nu_i = \left[\frac{1}{\left(\frac{\mathrm{Re}_S * \mathrm{Pr}}{2}\frac{S}{2L}\right)^3} + \frac{1}{\left(0.664\sqrt{\mathrm{Re}_S\cdot\frac{S}{2L}}\cdot \mathrm{Pr}^{1/3}\sqrt{1+\frac{3.65}{\sqrt{\mathrm{Re}_S\cdot\frac{S}{2L}}}}\right)^3}\right]^{-1/3} \qquad \textbf{(11)}$$

Pr: Prandtl Number, ν/α,
α : Thermal diffusivity, m^2/s
ν : Kinematic viscosity, m^2/s.

RESULTS AND DISCUSSIONS

Performance of Heatsinks

The performance curves of all the bonded (via swaging) heat sinks are shown in *Figures 7 and 8*. As expected, the all Copper (Cu B-Cu F) heatsink possessed the lowest thermal resistance while the all Aluminum (Al B-Al F) had the highest. In other words, the all Copper and all Aluminum sinks represented the limiting cases of performance. This behavior is explained by the higher thermal conductivity of the Copper as compared to the Aluminum, which results in lower thermal spreading resistance in the baseplate, better heat conduction through the fins and higher over all heat transfer to the ambient air.

Figures 7 & 8 show the thermal resistance of the tested heatsinks versus fin channel Reynolds number, Re_S. Figure 7 shows the thermal resistance of the heatsinks, R_θ, based on the average temperature of the ten temperature measurements on the baseplate as defined in equation 1. Figure 8 shows the source thermal resistance, $R_{\theta\,Source}$, based on the average value of the temperature measurements at the nearest locations to the block heater, T_{a1}, T_{a2}, T_{a3} and T_{a4} as shown in *Figure 6*. Due to the proximity of these four thermocouples with the heater block, the values of the thermal resistance in Figure 8 are higher than those in Figure 7.

With the Cu B-Al F heatsink, the Copper baseplate decreases the thermal spreading resistance in the baseplate, which in turn helps to decrease the over all thermal resistance of the heatsink. With the Al B–Cu F heatsink, the over all thermal resistance of the heatsink is decreased as the Copper used in the fins helps to increase the fin efficiency. Comparing the thermal performance of these two heatsinks from Figures 7 and 8, we can conclude that the thermal performance of the Al B–Cu F heatsink is better than the Cu B-AL F heatsink for small source coverage.

Table 2 shows the percentage reduction in thermal resistance for the alternative metal heat sinks with respect to the thermal resistance of the all Aluminum heat sink for the full range of Reynolds number. The all copper (Cu B-Cu F) heat sink has the lowest thermal resistance with up to 28.7% reduction in source thermal resistance , $\%R_{\theta\,Source}$.

Table 2: Thermal resistance comparison of alternative metal heat sink performance with respect to an all Aluminum heatsink.

Cu B - Al F			**Al B – Cu F**			**Cu B-Cu F**		
Re_S	$\%R_\theta$	$\%R_{\theta\,Source}$	Re_S	$\%R_\theta$	$\%R_{\theta\,Source}$	Re_S	$\%R_\theta$	$\%R_{\theta\,Source}$
742	0.1	6.6	743	3.0	6.0	751	12.5	19.4
1144	1.4	8.8	1155	9.3	11.4	1165	17.2	24.3
1554	3.0	10.7	1562	10.5	12.6	1571	17.0	24.6
1962	4.1	12.0	1971	11.7	13.6	1981	18.2	26.0
2370	4.5	12.6	2379	12.4	14.2	2392	19.6	27.4
2775	6.3	14.0	2787	13.0	14.6	2802	20.5	28.2
3190	6.4	14.4	3198	13.4	14.9	3214	21.0	28.7

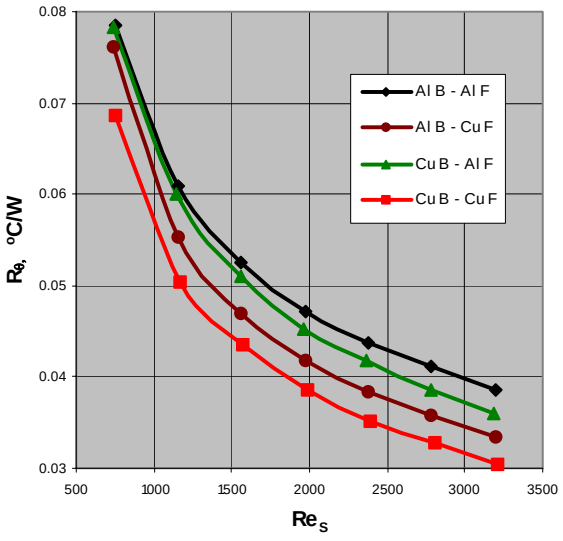

Figure 7: Thermal resistance based on average base plate temperature T_S vs. fin spacing Reynolds Number.

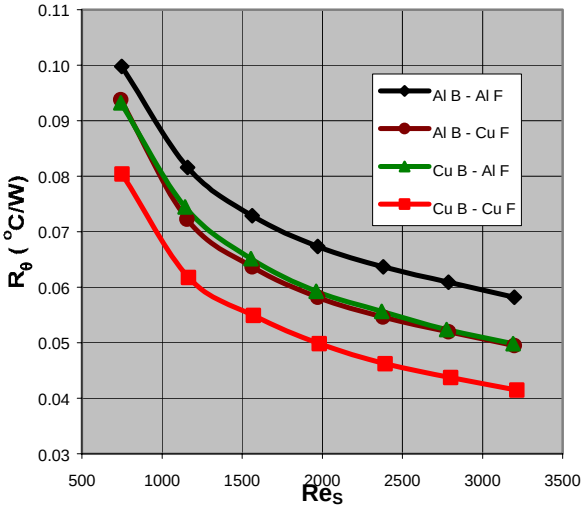

Figure 8: Thermal resistance based on the temperature measurements at the nearest locations of the block heater vs. fin channel Reynolds Number.

From Table 1, the average thickness of the flat Copper fins is 1.3 mm while the average thickness of the serrated Aluminum fins is 1.2 mm. Due to this difference in fin thickness, the fin spacing, S, of the Copper fins is 2.1mm while that of the serrated Aluminum fins is 2.23 mm. *Figure 9* shows that the pressure drop of the air going through the Copper fin heatsinks (Al B – Cu F & Cu B-Cu F) can be expected to be higher than when going through the serrated Aluminum fin heat sinks (Al B-Al F & Cu B-Al F).

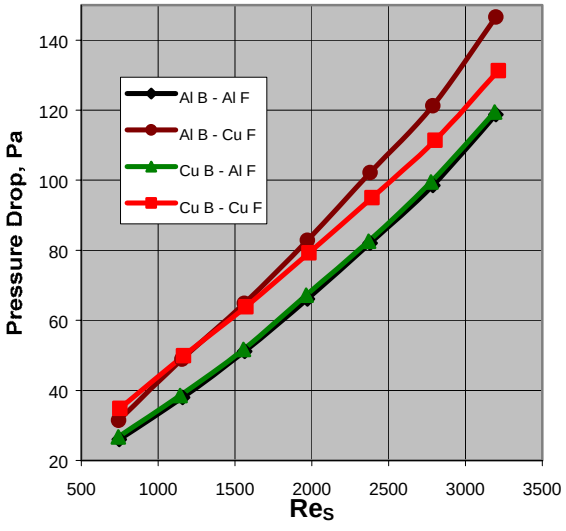

Figure 9: Pressure drop vs. fin channel Reynolds Number.

Experimental Results and Model Comparison

Figures 10 & 11 compare the experimental average Nusselt number [Eq. 9] with the Teertstra model [Eqs. 10 & 11] for the two limiting cases of the all Aluminum and all Copper heatsinks. Teertstra et al based their model on the assumption that the baseplate possessed a uniform temperature that was equal to the average of the measured values. During their testing, they found that the maximum difference between individual temperature measurements and the averaged value was below 15%.

Due to the small source coverage area in the experiments that this paper focuses on, the maximum difference in the temperature measurements from the mean value was significantly higher. For the all Aluminum heat sink, 34% was the maximum difference from the mean value while the maximum percentage difference in the temperature measured for the all Copper heatsink was 23%. The high conductivity Copper reduces the spreading resistance in the baseplate , which results in a more uniform baseplate temperature distribution. Figure 10 shows that the difference between the experimental Nusselt number and the model for the all Aluminum heatsink ranges from 4.6% at low Reynolds number to 18.8% for high Reynolds number (see Table 2). This deviation is expected due to the large temperature differences on the base plate. Figure 11 shows that the predicted Nusselt number values for the all Copper heatsink show good agreement with the experimental results. As seen in table 2, the maximum difference is within –3.5% and 7.2%.

In general, the model can predict the Nusselt number for small values of Reynolds number when the maximum temperature difference between the measured temperature and the heatsink average temperature is small. With increasing Reynolds number, the temperature distribution of the base plate will increasingly become non-uniform so that the difference between the experimental Nusselt number and the predicted values will also increase.

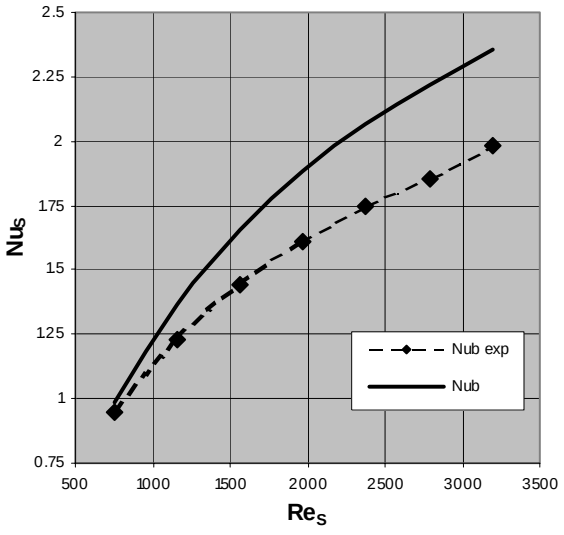

Figure 10: Nusselt number comparison of Teertstra et al model with measured values for all Aluminum (**Al B-Al F**) heatsink.

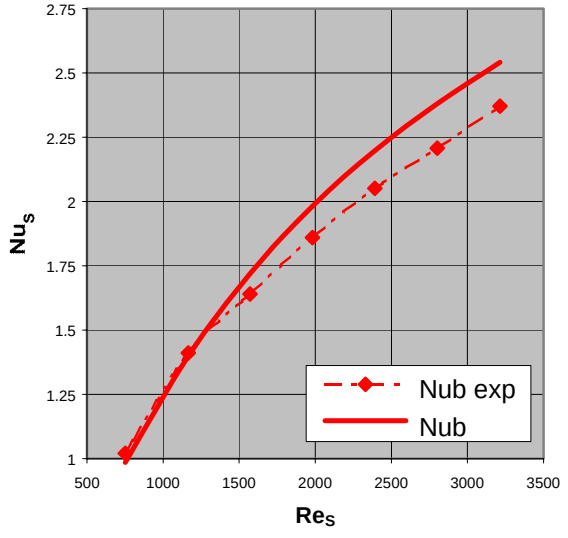

Figure 11: Nusselt number comparison of Teertstra et al model with measured values for all Copper (**Cu B-Cu F)** heatsink

CONCLUSIONS

The thermal performances of the four-heatsink combinations under forced convective heat transfer mode have been performed. The four designs comprise an Aluminum base/Aluminum fin (Al B-Al F), Copper base/Aluminum fin (Cu B-Al F), Aluminum base/Copper fin (Al B-Cu F) and Copper base/Copper fin (Cu B-Cu F) heatsinks. As expected, the all Copper (Cu B-Cu F) heatsink had the lowest thermal resistance with up to a 28.7% reduction in source thermal resistance as compared to the all Aluminum sink. However, the Copper heatsink possessed 3.5 times the weight of the Aluminum heatsink. Up to 15% reduction in thermal resistance was achieved by using a Copper base/Aluminum Fin (Cu B-Al F) or Aluminum base/Copper fin (Al B-Cu F) sink. The Cu B-Al F heatsink had the lowest weight increase being only twice as heavy as the all Aluminum heatsink.

The experimental average Nusselt number was compared with the Teertstra model. There was a difference of up to 16% between the experimental Nusselt number and the model for the all Aluminum heatsink due to the large temperature differences within the baseplate. The predicted Nusselt number values for the all Copper heatsink **Cu B-Cu F** showed good agreement with the experimental results with the maximum difference being within –3.5% to 7.2%

ACKNOWLEDGMENTS

The authors would like to acknowledge the financial support of Materials and Manufacturing Ontario. The authors also acknowledge the assistance of James Wong for preparation of figures.

REFERENCES

H.W. Chu, C.L. Belady and C.D. Patel, “A Survey of High-performance, High Aspect Ratio, Air Cooled Heat Sinks”, 1999 International Systems Packaging Symposium, Jan. 11-13, 1999, San Diego, California, USA.

H. Jonsson and B. Palm, “Influence of Airflow Bypass on the Thermal performance and Pressure Drop of Plate Fin and Pin Fin Heat Sinks for Electronics Cooling”, Proceedings of Eurotherm Sem. No. 58, Nantes, France, Sept. 24-26, 1997, pp. 44-50.

Robert W. Messler Jr., *Joining of Advanced Materials*, Stoneham, MA, 1993.

R-Theta Catalogues.

P. Teertstra, M.M. Yovanovich, J.R. Culham, and T. Lemczyk “Analytical Forced Convection Modeling of Plate Fin Heat Sinks”, Semi-Therm 15th IEEE Symposium, March 9-11, 1999, San Diego, California, USA.